Thermochimica Acta, 195 (1992) 211–220
Elsevier Science Publishers B.V., Amsterdam

Measurements of accurate specific heats of metallic glasses by differential scanning calorimetry (DSC).
Part 2. Specific heat of $Fe_{73}Co_{12}B_{15}$ metallic glass from 300 to 1054 K

E. Illeková [a], B. Aba [b] and F.A. Kuhnast [b]

[a] *Institute of Physics SAS, Dubravská cesta, 84228 Bratislava (Czechoslovakia)*
[b] *Laboratoire de Thermodynamique Métallurgique, Université de Nancy I, B.P. 239, 54506 Vandoeuvre-lès-Nancy Cedex (France)*

(Received 10 May 1991)

Abstract

The specific heat at constant pressure of $Fe_{73}Co_{12}B_{15}$ glassy ribbon in the as-quenched, relaxed and crystalline states was measured in the range 300–1054 K using DSC measuring techniques. The room temperature specific heat of the stable form of the ribbon is $c_{p(\text{crystalline})}$ (303 K) = 21.81 ∓ 0.40 J g-at^{-1} K^{-1}. The excess contributions due to the relaxed glassy state of the sample and to the structural relaxation of the glassy sample were +6.7% and +1.2%, respectively. In the medium temperature range, the linear $c_p(T)$ dependence of all three forms of the investigated ribbons was measured; the several anomalous transformation contributions represent the kinetics of the structural relaxation and crystallization heat generation effects.

INTRODUCTION

Metallic glasses prepared by rapid quenching are thermodynamically metastable with respect to both the corresponding crystalline and the glassy structures. Processes taking place in the glassy structure are usually explained in terms of changes of short range ordering (SRO). Until now no unambiguous mechanism has been proposed to explain these processes. It is supposed that there exist two types of short range ordering in the glassy structure, namely TSRO (topological) and CHSRO (chemical).

The present study concentrates on measuring the temperature dependence of specific heat capacity (specific heat) of an $Fe_{73}C_{12}B_{15}$ glassy ribbon in the range 300–1054 K using four DSC methods. The scanning and integral methods tested in our previous article [1] are also used. The aim of these experiments was to obtain and analyze the thermodynamic data, which are still scarce [2–4].

EXPERIMENTAL

The $Fe_{73}Co_{12}B_{15}$ metallic glassy ribbon was prepared by rapid quenching using a single roller casting apparatus. The ribbon had the dimensions 35 μm × 10 mm × several meters.

The technique of DSC was used to investigate the temperature dependence of specific heat $c_p(T)$ of glassy ribbons. The power-compensated Perkin–Elmer DSC7 with PE 3700 Data Station, as well as the heat-flux SETARAM DSC111 with a Commodore Data Station, were used.

Four main principal representations of measured DSC data were studied. These are: (1) heat-power thermograms measured on the PE DSC in the continuous heating regime, (2) heat-flux thermograms measured on the SETARAM DSC in the continuous heating regime, (3) the specific heats measured and calculated by the scanning (differential) method using the PE DSC in a continuous heating regime and the PE DSC7 specific heat software, and (4) the specific heats measured and calculated by the integral (enthalpic) method using the SETARAM DSC in a discontinuous (stepwise) heating regime and special software [5].

The theoretical principles of DSC techniques and of the scanning and integral data acquisition methods were described in our previous article [1].

To characterize the three limiting forms of a metallic glass: (a) the so-called as-quenched (not heat treated) state, (b) the ideally relaxed (not changing after any other heat treatment, and avoiding crystallization) state, and (c) the final stable crystalline state of the sample, three successive heating runs of equivalent measurements were necessary (designated 1st, 2nd and 3rd runs) followed by reproducible cooling of the sample without breaking off the measurement. The previous DSC investigations at heating rates $w = 40$, 20, 10 and 2 K min^{-1} [6] have defined the 5-fold repeated continuous heating regime ($w = 10$ K min^{-1}) to $T_{\text{final}} = 340$ K combined with rapid cooling ($w = -200$ K min^{-1}) after the first and before the second measuring runs.

The heating rates w used in measurements of types (1) and (2) were 2–40 K min^{-1}. The optimal heating rate was $w = 5$ K min^{-1} in measurements of type (3) and $w = 5$ K min^{-1} for 200 s followed by stabilization isothermal periods of 400 s (the quasi-linear mean heating rate $\bar{w} = 1.6$ K min^{-1}) in the discontinuous stepwise heating regime in experiments of type (4).

The masses investigated in the PE DSC were $m \approx 50$ mg, and in the SETARAM DSC $m \approx 360$ mg. The samples were cut into small pieces. The reference in the PE DSC was always an empty Al pan, and that in the SETARAM DSC was an empty Al_2O_3 pan. All measurements were made in an argon atmosphere.

RESULTS

Four representations of $c_p(T)$ dependences of measured DSC data were obtained: (1), shown in Figs. 1, 2 and 6; (2), Fig. 3; (3), Figs. 4 and 5; (4), Fig. 4.

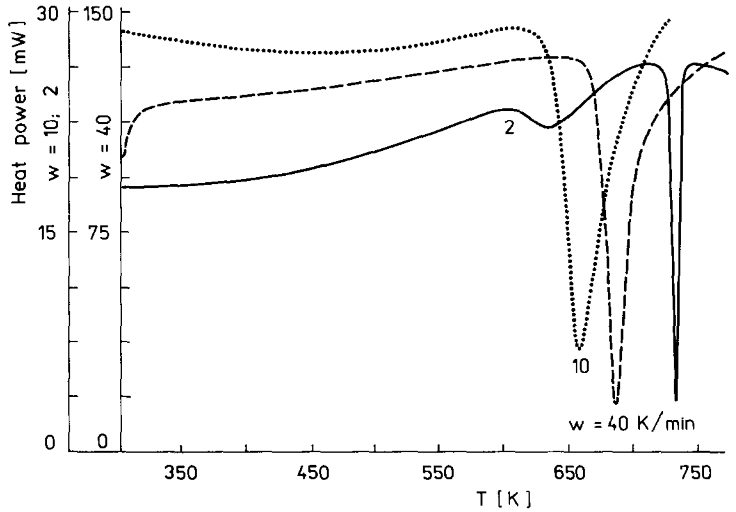

Fig. 1. Influence of the heating rate w on the heat-power $\Delta J_{(M-R)}(T)$ representation of PE DSC thermograms of an as-quenched $Fe_{73}Co_{12}B_{15}$ glassy ribbon.

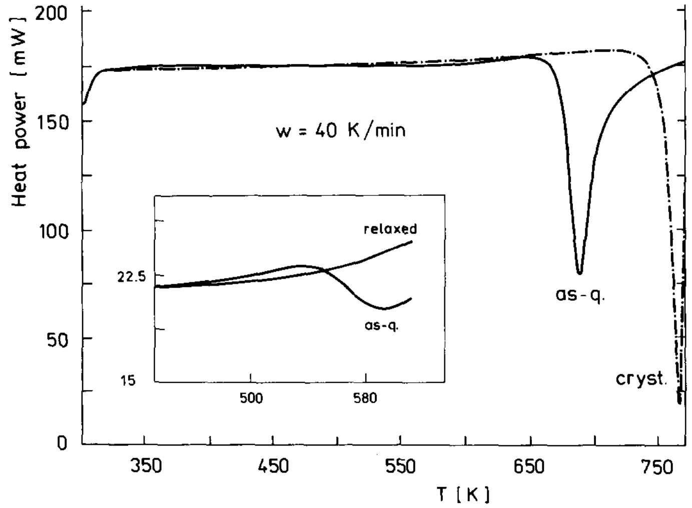

Fig. 2. The heat-power representation of PE DSC thermograms of as-quenched and partially crystallized $Fe_{73}Co_{12}B_{15}$ glassy ribbons ($w = 40$ K min^{-1}). In detail, the relation between the as-quenched (1st run) and relaxed (2nd run) glassy ribbons [6].

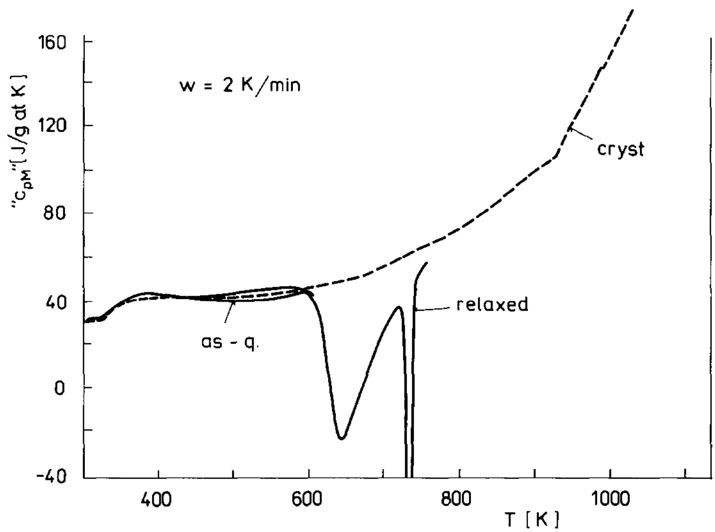

Fig. 3. SETARAM continuous heating thermograms of as-quenched (1st run), relaxed (2nd run) and crystallized (3rd run) $Fe_{73}Co_{12}B_{15}$ glassy ribbons.

The examples of typical heat-power $\Delta J_{(M-R)}(T)$ thermograms (where M and R mean the measured and reference samples respectively) measured on the PE DSC are in Figs. 1, 2 and 6. The analysis of the complex anomalous behavior of such a representation of $c_p(T)$, having one pronounced structural relaxation exotherm and some possible endotherms followed by several crystallization exotherms, and of the influence of heat treatment on it was carried out in [6].

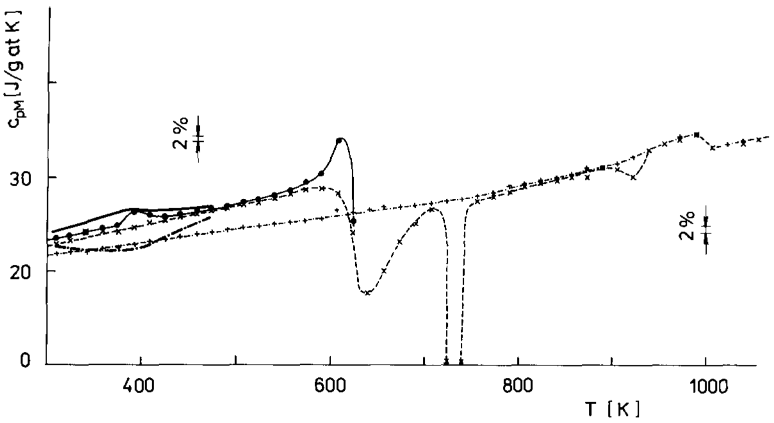

Fig. 4. Temperature dependence of mean apparent specific heat $c_{pM}(T)$ of $Fe_{73}Co_{12}B_{15}$ glassy ribbon: (●) as-quenched; (×) relaxed; (+) crystalline, measured by SETARAM DSC and integral method ($\bar{w} = 1.6$ K min^{-1}) (———) as-quenched; (–·–·–) crystalline, measured by PE DSC and scanning method ($w = 5$ K min^{-1}).

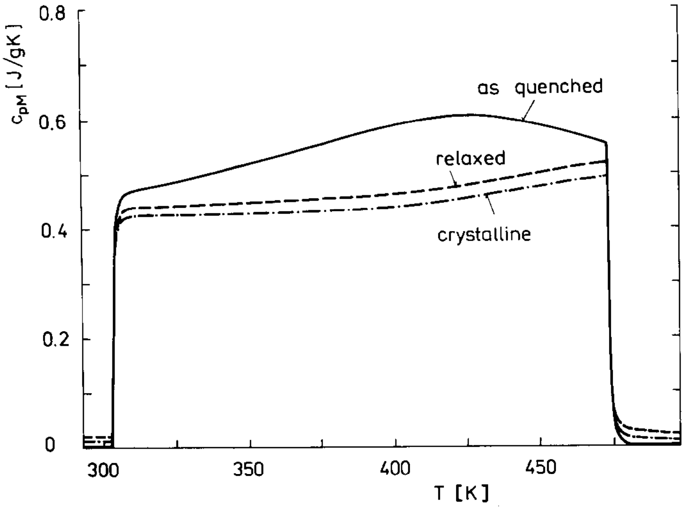

Fig. 5. Temperature dependence of apparent specific heat $c_{pM}(T)$ of an $Fe_{73}Co_{12}B_{15}$ glassy, relaxed and crystalline ribbon sample measured by PE DSC and scanning method ($w = 5$ K min^{-1}).

Equivalent continuous heating regime thermograms measured on the heat-flux SETARAM DSC are in Fig. 3. The ordinates $c_{pM}(T)$ of the thermograms are the measured signals $\Delta T_{(M-R)}$ recalculated to the specific heat dimensions by means of the specified instrumental sensitivity coefficient $K \approx 1/(m_M w)$, where m_M is the mass of the sample.

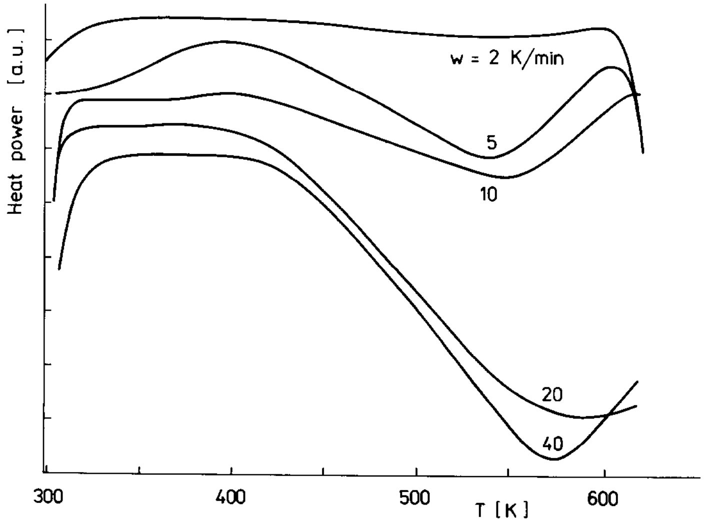

Fig. 6. Influence of heating rate w on structural relaxation anomalies of specific heat of as-quenched $Fe_{73}Co_{12}B_{15}$ glassy ribbon (in a heat-power representation of PE DSC by subtracted (1st run – 2nd run) thermograms.

TABLE 1

Mean values of specific heat $c_{pM}(303\ \mathrm{K})$ in J g-at^{-1} K^{-1} of a $Fe_{73}Co_{12}B_{15}$ metallic glassy ribbon

Method	As-quenched	Relaxed	Crystalline	$\Delta c_{p(\text{as-q}-\text{rel})}$	$\Delta c_{p(\text{as-q}-\text{cryst})}$
Theoretical [7]			22.87		
SETARAM	23.55 ∓ 0.61	23.28 ∓ 0.04	21.81 ∓ 0.40	$+0.28$	$+1.74$
(integral)	$\mp 2.5\%$	$\mp 0.2\%$	$\mp 1.8\%$	$+1.2\%$	$+7.4\%$
PE	24.20 ∓ 0.48	23.90	22.53 ∓ 0.38	$+0.30$	$+1.67$
(scanning)	$\mp 2.0\%$		$\mp 1.9\%$	$+1.2\%$	$+6.9\%$

TABLE 2

Mean values of specific heat $c_{pM}(468\ \mathrm{K})$ in J g-at^{-1} K^{-1} of a $Fe_{73}Co_{12}B_{15}$ metallic glassy ribbon

Method	As-quenched	Relaxed	Crystalline	$\Delta c_{p(\text{as-q}-\text{rel})}$	$\Delta c_{p(\text{as-q}-\text{cryst})}$
SETARAM	26.40 ∓ 0.20	26.30 ∓ 0.06	23.97 ∓ 0.69	$+0.10$	$+2.43$
(integral)	$\mp 0.8\%$	$\mp 0.2\%$	$\mp 0.9\%$	$+0.4\%$	$+9.2\%$
PE	26.97 ∓ 0.61	26.22	25.22 ∓ 0.41	$+0.75$	$+1.75$
(scanning)	$\mp 2.3\%$		$\mp 1.6\%$	$+2.8\%$	$+6.5\%$

Accurate absolute values of $c_p(T)$ for the investigated ribbons were measured and calculated by the discontinuous heating regime of the SETARAM DSC and the integral method, as well as by the continuous heating regime of the PE DSC and the scanning method. Some examples of the $c_p(T)$ dependences are seen in Figs. 4 and 5. Analyses of the theoretical principles and errors of measured $c_p(T)$ data have been carried out in [1].

The absolute values of $\overline{c_p(303\ \mathrm{K})}$ and $\overline{c_p(468\ \mathrm{K})}$ and their errors for as-quenched, relaxed and crystalline $Fe_{73}Co_{12}B_{15}$ ribbons, obtained by both measuring techniques (3) and (4), are compared in Tables 1 and 2. They can be related to a hypothetical theoretical $c_{p(\text{theoret.},Fe_{73}Co_{12}B_{15})}(308\ \mathrm{K}) = 22.87$ J g-at^{-1} K^{-1}, which was calculated by means of the Kopp–Neumann law, which supposed the heat capacity of an equilibrium crystalline alloy to be the mean value of the weighted heat capacities of its elements [7].

DISCUSSION

Let us try to analyze qualitatively the various contributions to the total measured apparent specific heat $c_{pM}(T)$ of our samples.

The steady state $c_p(T)$ *dependence*

As can be expected from a few previous studies of metallic glasses like, e.g., $Au_{18.6}Si_{81.4}$ [2], $Ni_{40}Pd_{40}P_{20}$ [3] or $Fe_{78}Si_9B_{13}$ [4], the absolute $c_{pM}(T)$

values of as-quenched, relaxed and crystalline $Fe_{73}Co_{12}B_{15}$ samples are similar. The room temperature apparent specific heat of an as-quenched sample is relatively high—$c_{p(\mathrm{SETARAM})}(303\ \mathrm{K}) = 23.55 \mp 0.61$ J g-at^{-1} K^{-1}; it is lowered by about 1.2% because of the structural relaxation and further by 6.2% owing to crystallization.

Excluding the excess anomalies, $c_p(T)$ values exhibit linear temperature dependences. For the medium temperature region they were fitted with polynomials in temperature by the method of least squares

$$c_{p(\text{as-quenched})}(T) = 17.64 + 1.94 \times 10^{-2}T \text{ in J g-at}^{-1}\ \mathrm{K}^{-1} \quad \text{for } T = 304\text{–}557\ \mathrm{K} \tag{1}$$

$$c_{p(\text{relaxed})}(T) = 16.77 + 2.05 \times 10^{-2}T \quad \text{for } T = 304\text{–}557\ \mathrm{K} \tag{2}$$

$$c_{p(\text{crystalline})}(T) = 17.56 + 1.39 \times 10^{-2}T \quad \text{for } T = 407\text{–}756\ \mathrm{K} \tag{3}$$

At temperatures $T > 780$ K, $c_p(T)$ values of the relaxed (2nd run) and crystalline (3rd run) samples almost coincide (Fig. 4).

The major part of the heat capacity C_p of transition metals (which make up the investigated metallic glassy alloy) is given by the harmonic vibrational heat capacity [8]. It approaches asymptotically the value $C_v \approx 3R$ per g-atom at high temperatures. At intermediate temperatures, this term is well described by a Debye or Einstein model, $C_v \approx T^3$.

There are more heat capacity contributions, which are linear in T, to the leading order. First of all there is the dilation heat capacity term described by the quasi-harmonic model to be $C_d = C_p - C_v \approx \beta^2 VT/\chi$, where β is the isobaric expansivity, V is the g-atomic volume, and χ is the isothermal compressibility.

The other terms are the explicit anharmonic contributions to C_v, which can have any sign ($C_{v,a} \approx T$) and the electronic heat capacity, which is less dominant at room temperature: $C_{el} = \gamma T$; γ is the electronic heat capacity coefficient.

Because there is a lack of data on β, χ, γ, vibrational spectra, lattice parameters and their dependences on thermal history, it is not possible to separate quantitatively the different terms. Only a qualitative conclusion can be drawn: the atom lattice vibrational spectra, the specific volumes and the expansion and compressibility properties of as-quenched, relaxed and crystalline $Fe_{73}Co_{12}B_{15}$ ribbons do not change too much (this correlates well with the fact of existence of some short range ordering in the glassy structure related to the crystalline one), and the Debye temperature $T_D < 300$ K.

Transformation contributions to $c_{pM}(T)$

If in the sample some transformation occurs, two contributions to the measured specific heat occur.

(1) The specific heat c_p at temperature T evolves with time

$$c_p(T,t) = [1 - \alpha(T,t)]c_{p1}(T) + \alpha(T,t)c_{p2}(T) \tag{4}$$

where c_{p1} and c_{p2} are magnitudes of the specific heats of the initial and final phases.

(2) At each temperature the excess heat capacity $\mathrm{d}H/\mathrm{d}T$ due to the thermal effect occurring in the sample is

$$\frac{\mathrm{d}H(T,t)}{\mathrm{d}t} = \frac{\mathrm{d}\alpha(T,t)}{\mathrm{d}T}\Delta H \tag{5}$$

where α is the degree of transformation, fulfilling a reasonable kinetic equation, and ΔH is the enthalpy change of the transformation.

Then the measured apparent specific heat of a sample is

$$c_{p\mathrm{M}}(T,t) = c_p(T,t) + \frac{\mathrm{d}H(T,t)}{\mathrm{d}T}\frac{1}{m_\mathrm{M}} \tag{6}$$

Knowing the $c_{p1}(T)$ and $c_{p2}(T)$ dependences of the starting and final (i.e. glassy and crystalline) phases, $c_{p(\mathrm{glass})}(T)$ [defined by eqn. (1)] and $c_{p(\mathrm{crystal})}(T)$ [defined by eqn. (3)], and measuring the $c_{p\mathrm{M}}(T)$ dependence [in our case the $c_{p(\mathrm{PE})}(T)$ in Figs. 4 and 5, approximately the thermograms in Figs. 1–3 and 6, but in the case of the mean $c_{p(\mathrm{SETARAM})}(T)$ in Fig. 4 the kinetic information is only schematic], the $\alpha(T,t)$ dependence can be determined. Then the corresponding kinetic equation can be solved, the kinetic parameters of the sample calculated and the mechanism of transformation identified.

Such kinetic relationships are the basis of many classical kinetic investigations of metallic glasses by the use of DSC techniques e.g., refs. 9–11. Our thermodynamic stability and kinetic analyses of glassy $\mathrm{Fe_{73}Co_{12}B_{15}}$ using the differential non-isothermal Kissinger method and the assumption of JMA nucleation-growth mechanism of crystallization [12] gave the enthalpies and activation energies for the first and second crystallization exotherms to be $\Delta H_{\mathrm{cr1}} \approx 96$ kJ g-at^{-1}, $\Delta H_{\mathrm{cr2}} \approx 86$ kJ g-at^{-1}, $\Delta E^*_{\mathrm{cr1}} \approx 179$ kJ g-at^{-1}, $\Delta E^*_{\mathrm{cr2}} \approx 256$ kJ g-at^{-1}, which correlate well with the results from the isothermal Avrami method [13].

Phase analysis of measured anomalies of $c_{pM}(\mathrm{T})$

There are several anomalies on the apparent specific heat temperature dependence $c_{p\mathrm{M}}(T)$ in Fig. 4.

The main structural relaxation exotherm ($\Delta H_{\mathrm{relax}} \approx 500$ J g-at^{-1}) characterizing the reduction of excess free volume at $T > 400$ K and several anneal-induced (in the course of the first and second runs) endotherms (fig. 7 in ref. 6, or e.g. Figs. 2 and 6 in this article) at $T > 500$ K are not seen well on these scales (because of the relatively small heating rates used), excluding the glass transition anomaly at about 600 K, which continues very quickly to the more complicated stage of crystallization.

The electron microscopy phase analysis of crystallization of a $Fe_{73}Co_{12}B_{15}$ glassy ribbon is reminiscent of that of $Fe_{85}B_{15}$ [14]. The Co content of 12 at% does not impose any phase preference, but it replaces some Fe atoms in the basic binary $Fe_{85}B_{15}$ glassy system.

There is a characteristic asymmetric exotherm which corresponds to polymorphous crystallization of supersaturated α-Fe glassy regions (about 50% of the sample mass) above 600 K. This is followed by a relatively brief crystallization exotherm above 700 K, which represents the α-Fe crystallization of the remaining amorphous regions absorbing the parts crystallized before, together with precipitation of Fe_3B. The crystallization process is completed by recrystallization to Fe_2B above 900 K. At about 1000 K a Curie point anomaly of crystalline iron can be seen.

It is generally known that both the structural relaxation and the crystallization $c_{pM}(T)$ anomalies are strongly dependent on the measuring regime (Figs. 1 and 6). This might explain the discrepancies in the PE and SETARAM representations of $c_{pM}(T)$ of an as-quenched glassy sample in Fig. 4.

There is an interesting endothermic anomaly having a maximum at about 400 K for the as-quenched sample, which could be seen only at a heating rate of 5 K min^{-1} (related curves on Figs. 4–6). On the base of our analysis of heat treatment influence on the $c_{pM}(T)$ dependence of the glassy samples investigated in [6] we suppose that it might be anneal induced during aging of the sample (for 2 years at room temperature) and during the course of the first run. This endotherm does not have a very reproducible position or enthalpy (see fig. 5 in ref. 1), which could be attributed to some local thermodynamic properties of the sample.

CONCLUSIONS

It seems reasonable to conclude that the measured room temperature specific heat c_{pM} of an as-quenched, relaxed and crystalline $Fe_{73}Co_{12}B_{15}$ ribbon does not change very much. The structural configurational terms $\Delta c_{p(\text{as-quenched}-\text{relaxed})}$ (303 K) or $\Delta c_{p(\text{as-quenched}-\text{crystalline})}$ (303 K) make contributions of +1.2 or +7.4%. The specific heat of the stable crystalline form of the ribbon is $c_{p(\text{crystalline})}(303\ K) = 21.81 \mp 0.40$ J $g\text{-}at^{-1}\ K^{-1}$.

On increasing the temperature two different thermal events occur: (a) a quasi-linear temperature dependent evolution of $c_p(T)$ according to eqns. (1)–(3) for all three forms of the investigated ribbon, (b) several anomalous heating rate dependent endothermal and exothermal effects at $T < 600$ K related to the influence of thermal history on structural relaxation, multistage crystallization and recrystallization of the glassy sample at $T > 600$ K and a Curie point at $T \approx 1000$ K.

A qualitative coincidence of the four sets of thermograms and also quantitative correspondence of two sets of measured $c_M(T)$ dependences was evident. The advantages of the correct scanning and integral methods for measuring the accurate $c_{pM}(T)$ dependences of metallic ribbons by means of DSC instruments are their simplicity, commercial availability and high productivity.

ACKNOWLEDGEMENTS

The authors thank Dr. P. Duhaj for his interest and for the electron microscopy phase analysis of the crystallization of a $Fe_{73}Co_{12}B_{15}$ glassy ribbon, and express appreciation of the assistance of Dr. J. Šesták in communicating the article to Thermochimica Acta.

REFERENCES

1 For Part I see E. Illeková, B. Aba and F.A. Kuhnast, Thermochim. Acta, 195 (1992) 195.
2 H.S. Chen and D. Turnbull, J. Appl. Phys., 38 (1967) 3646.
3 H.W. Kui and D. Turnbull, J. Non-Cryst. Solids, 94 (1987) 62.
4 R.J.J. Martis, T.J. Taylor and Y.P. Khanna, J. Non-Cryst. Solids, 94 (1987) 209.
5 C. Cunat and J. Charles, Mem. Sci. Rev. Metall., 79 (1982) 177.
6 E. Illeková, C. Cunat, F.A. Kuhnast, A. Aharoune and J.M. Fiorani, Thermochim. Acta, to be published.
7 I. Barin, O. Knackle and O. Kubaschewski, Thermodynamical Properties of Inorganic Substances, Supplement, Springer-Verlag, Berlin, 1977.
8 G. Grimvall, in E.P. Wohlfarth (Ed.), Thermophysical Properties of Materials, North-Holland, Amsterdam, 1986, p. 174.
9 E. Illeková, P. Ambrovič and P. Duhaj, J. Therm. Anal., 28 (1983) 413.
10 E. Illeková, J. Non-Cryst. Solids, 68 (1984) 153.
11 E. Illeková, Acta Phys. Slov., 34 (1984) 255.
12 J.M. Fiorani, F.A. Kuhnast and C. Cunat. Proc. AFCAT Conf. 1990, to be published.
13 S. Budurov, M. Lazarova and E. Illeková, in P. Duhaj, P. Mrafko and P. Švec (Ed.), Proc. 2nd Int. Conf. Amorphous Metallic Materials, 2nd, Smolenice 1989, Vols. 40 and 41, Key Engineering Materials, Trans. Tech. Publications, Zürich, 1990, pp. 93–99.
14 P. Duhaj, P. Švec and G. Vlasák, in S. Steeb and H. Warlimont (Ed.), Proc. 5th Conf. Rapidly Quenched Metals, Würzburg, 1984, North-Holland, Amsterdam, 1984, pp. 271–275.